



1 Enhanced Mediterranean water cycle
2 explains increased humidity during MIS 3
3 in North Africa
4

5 Mike Rogerson¹

6 Yuri Dublyansky²

7 Dirk L. Hoffmann³

8 Marc Luetscher^{2,4}

9 Christoph Spötl²

10 Paul Töchterle²

11 1 School of Environmental Sciences, University of Hull, Cottingham Road, Hull, HU6 7RX, UK.

12 2 Institute of Geology, University of Innsbruck, Innrain 52, 6020 Innsbruck, Austria.

13 3 Department of Human Evolution, Max Planck Institute for Evolutionary Anthropology, Deutscher
14 Platz 6, 04103, Leipzig, Germany

15 4 Swiss Institute for Speleology and Karst Studies (ISSKA), Serre 68, CH-2300 La Chaux-de-Fonds

16



17 Abstract

18 *We report a new fluid inclusion dataset from Northeast Libyan speleothem SC-06-01, which is the*
19 *largest speleothem fluid inclusion dataset for North Africa to date. The stalagmite was sampled in*
20 *Susah cave, a low altitude coastal site, in Cyrenaica, on the northern slope of the Jebel Al-Akhdar.*
21 *Speleothem fluid inclusions from latest Marine Isotope Stage (MIS) 4 and throughout MIS 3 (~67 to*
22 *~30 ka BP) confirm the hypothesis that past humid periods in this region reflect westerly rainfall*
23 *advected through the Atlantic storm track. However, most of this moisture was sourced from the*
24 *Western Mediterranean, with little direct admixture of water evaporated from the Atlantic. Moreover,*
25 *we identify a second moisture source likely associated with enhanced convective rainfall within the*
26 *Eastern Mediterranean. The relative importance of the western and eastern moisture sources seems to*
27 *differ between the humid phases recorded in SC-06-01. During humid phases forced by precession,*
28 *fluid inclusions record compositions consistent with both sources, but the 52.5 – 50.5 ka interval*
29 *forced by obliquity reveals only a western source. This is a key result, showing that although the*
30 *amount of atmospheric moisture advections changes, the structure of the atmospheric circulation over*
31 *the Mediterranean does not fundamentally change during orbital cycles. Consequently, an arid belt*
32 *must have been retained between the Intertropical Convergence Zone and the mid-latitude winter*
33 *storm corridor during MIS 3 pluvials.*

34 Introduction

35 Atmospheric latent heat is a major component of global and regional climate energy budgets and
36 changes in its amount and distribution are key aspects of the climate system (Pascale et al., 2011).
37 Equally, in mid- and low-latitude regions, changes in the water cycle have more impact on landscapes
38 and ecosystems than changes in sensible heat (Black et al., 2010). Rainfall in semi-arid regions is thus
39 one of the key climate parameters that understanding future impact on human societies depends upon
40 (IPCC, 2014), making constraining of mid-latitude hydrology a globally significant research priority.
41 These regions, however, have a particularly sparse record of palaeoclimate due to typically poor
42 preservation of surface sedimentary archives (Swezey, 2001). North Africa is a region that fully



43 exhibits these limitations, and large areas present either no pre-Holocene record or else they present
44 highly discontinuous deposits indicating major reorganisation of the hydroclimate, which are
45 challenging to date (Armitage et al., 2007). North Africa also fully exhibits the progress
46 palaeoclimatologists have made in understanding continental hydrological change from its impact on
47 the marine system; our understanding of past North African hydroclimate is disproportionately drawn
48 from records from the Mediterranean Sea (Rohling et al., 2015) and the eastern Central Atlantic
49 (Goldsmith et al., 2017; deMenocal et al., 2000.; Adkins et al., 2006).

50

51 **Past changes in North African hydroclimate**

52 Marine-based evidence offers a coherent model in which changes in the spatial distribution of
53 insolation alter atmospheric circulation on orbital timescales (10^4 to 10^5 years) and force major
54 reorganisations of rainfall in semi-arid regions such as the Sahel and southern Saharan regions
55 (Rohling et al., 2015; Goldsmith et al., 2017). This result is at least partially confirmed in climate
56 modelling experiments (Bosmans et al., 2015; Tuenter et al., 2003) and provides a conceptual
57 framework in which fragmentary evidence of hydrological change on the adjacent continent can be
58 understood (Rowan et al., 2000). There is 1) strong geochemical evidence that runoff from the
59 African margin initiated the well-known “sapropel” thermohaline crises of the eastern Mediterranean
60 (Osborne et al., 2010; Osborne et al., 2008) and, 2) convincing evidence that the southern margin of
61 the Mediterranean was more variable than the northern in terms of the relative magnitude of
62 precipitation changes and the distribution of flora, fauna and hominid populations (Drake et al., 2011).
63 However, we emphasise the fact that this understanding is largely drawn from evidence from outside
64 continental North Africa, and that this limits our knowledge about the nature and impact of
65 hydrological changes in this region.

66 There is strong evidence for a more humid climate throughout the Sahara and Sahel regions during the
67 early Holocene (Gasse and Campo, 1994; Gasse, 2002; Fontes and Gasse, 1991; Prentice and Jolly,
68 2000; Jolly et al., 1998; Collins et al., 2017), and in older interglacial periods (Drake et al.,



69 2008;Armitage et al., 2007;Vaks et al., 2013). This evidence has been interpreted to indicate that
70 humid conditions extended from the modern Sahel (~15°N) to the Mediterranean coast (30-35°N).
71 However, this only partially agrees with model results, which do indicate orbitally forced migration of
72 the monsoon belt but not across such a large spatial scale as suggested by the empirical data. Model
73 experiments indicate that monsoonal rainfall occurring within the Intertropical Convergence Zone
74 (ITCZ) likely extended no further north than ~23°N (Harrison et al., 2015). This well-recognised lack
75 of agreement between rainfall fields in model experiments for the past and reconstructed
76 hydrographies from the distribution of lakes and vegetation (via pollen) (Peyron et al., 2006) remains
77 an major research problem. While some models also suggest that during times of high Northern
78 Hemisphere insolation, enhanced westerlies advected Atlantic moisture into the basin (Brayshaw et
79 al., 2009;Tuenter et al., 2003;Bosmans et al., 2015), high-resolution regional modelling indicates that
80 this primarily affected the northern Mediterranean margin only (Brayshaw et al., 2009). This result is
81 consistent with evidence of enhanced runoff at these times from the southern margin of Europe
82 (Toucanne et al., 2015). On the African coast east of Algeria, the southern limit of enhanced
83 precipitation arising from increased westerly activity within model experiments essentially lies at the
84 coastline (~32°N), and does not appear to drive terrestrial hydrological changes. Overall, there is
85 therefore a striking mismatch between the apparent humidity of Africa between 23 and 32°N in the
86 empirical record (a zonally oriented belt ~1000 km in width) and the climate models. This region
87 encompasses southern Tunisia, in which multiple lines of evidence for distinct and widespread
88 periods of increased humidity provide a highly secure basis for enhanced rainfall during Northern
89 Hemisphere insolation maxima (Ballais, 1991;PETIT-MAIRE et al., 1991), the Fezzan basin, in
90 which compelling evidence for multiple lake highstands exists (Drake et al., 2011) and western Egypt,
91 where large tufa deposits attest to higher past groundwater tables (Smith et al., 2004).

92 It is unlikely that significant further progress will be made in understanding the palaeoclimate of
93 North Africa without new empirical evidence of regional hydrological changes from which
94 atmospheric dynamics can be delineated.



95 **The central North African speleothem record**

96 Speleothem palaeoclimatology has high potential for North Africa, but is only recently becoming
97 established through key records developed for Morocco (Wassenburg et al., 2013; Ait Brahim et al.,
98 2017; Wassenburg et al., 2016). Until recently, the only speleothem record published from central
99 North Africa was a single continuous record from 20 to 6 ka BP from northern Tunisia (Grotte de la
100 Mine). This record shows a large deglacial transition in both $\delta^{13}\text{C}$ and $\delta^{18}\text{O}$ (Genty et al., 2006), with
101 oxygen isotopes indicating a 2-step change from a relatively isotopically heavy (-5‰) LGM (20-16 ka
102 BP), through an intermediate (-6 to -7‰) deglacial period (16-11.5 ka BP) to a relatively isotopically
103 light early Holocene. The $\delta^{13}\text{C}$ record indicates cool periods exhibiting higher carbon isotope values,
104 more clearly delineating the Bølling-Allerød / Younger Dryas oscillation than $\delta^{18}\text{O}$. This is assumed
105 to reflect higher soil respiration during warm periods (Genty et al., 2006). A major change in the
106 carbon isotopic composition occurred across the transition from the relatively arid glacial to the more
107 humid Early Holocene, and indicates a significant reorganisation of the regional hydroclimate.

108 However, it is difficult to interpret these data in isolation. A recently reported speleothem record (SC-
109 06-01) indicates that conditions in northern Libya during Marine Isotope Stage 3 (MIS 3) were more
110 humid than today, and shows isotopic evidence of a teleconnection between temperature in Greenland
111 and rainfall at the southern Mediterranean margin (Hoffmann et al., 2016). The oxygen isotope record
112 indicates that the water dripping into the cave during MIS 3 was isotopically too heavy for the
113 moisture to be sourced from within the monsoon system (Hoffmann et al., 2016). However, beyond
114 ruling out a southern source $\delta^{18}\text{O}_{\text{cc}}$ values alone are not sufficient to determine the origin of
115 atmospheric vapour. Three distinct humid phases within MIS3 are reported from this speleothem: 65-
116 61 ka, 52.5-50.5 ka and 37.5-33 ka. Phases I and III occur during times of low precession, when
117 summer insolation on the northern hemisphere is relatively increased. Phase II represents the first
118 evidence for high obliquity being able to cause a pluvial period in the north African subtropics in the
119 same manner as precession (Hoffmann et al., 2016). In SC06-01, all three growth phases are fractured
120 into multiple short periods of growth, and show a marked temporal coherence with Greenland



121 Dansgaard-Oeschger interstadials (Hoffmann et al., 2016). Here, we report fluid inclusion data from
122 this speleothem and discuss how this helps resolve some of the issues discussed above.

123 Speleothem fluid inclusions are small volumes of water that were enclosed between or within calcite
124 crystals as they grew, ranging in size from less than 1 μm to hundreds of μm (Schwarcz et al., 1976).
125 This water represents quantities of ancient drip-water that can be interrogated directly to ascertain the
126 isotopic properties of the oxygen ($\delta^{18}\text{O}_{\text{f}}$) and hydrogen ($\delta^2\text{H}_{\text{f}}$) it comprises. This powerful approach
127 circumvents some of the uncertainty inherent in the interpretation of the stable isotopic values
128 preserved in the calcite comprising the speleothem itself ($\delta^{18}\text{O}_{\text{cc}}$, $\delta^{13}\text{C}_{\text{cc}}$). Fluid inclusion isotopes have
129 been used to demonstrate changes in air temperatures (Wainer et al., 2011; Meckler et al.,
130 2015; Arienzo et al., 2015) and in the origin of the moisture from which precipitation was sourced
131 (McGarry et al., 2004; Van Breukelen et al., 2008). Fluid inclusions from speleothems in Oman have
132 also been used to identify monsoon-sourced precipitation during interglacial phases (Fleitmann et al.,
133 2003), providing a rationale for similar investigation of fluid inclusion isotope behaviour in North
134 Africa.

135 Material and Methods

136 SC-06-01 is a 93-cm long stalagmite from Susah Cave (Fig. 1, 32°53.419' N, 21°52.485' E), which
137 lies on a steep slope ~200 m above sea level in the Al Akhdar massif in Cyrenaica, Libya (Fig. 1). The
138 region is semi-arid today, with mean annual temperature ~20°C and receiving less than 200 mm
139 precipitation per year, mostly in the winter (October to April). The Al Akhdar massif has thin soil
140 cover and a Mediterranean “maquis” vegetation. Susah Cave is hydrologically inactive today, and all
141 formations are covered with dust. The chronology of the speleothem and the general features of its
142 growth and $\delta^{18}\text{O}_{\text{cc}}$ record are published elsewhere (Hoffmann et al., 2016), and this study focuses on
143 fluid inclusion isotopes, their impact on the interpretation of $\delta^{18}\text{O}_{\text{cc}}$ and to a lesser extent on $\delta^{13}\text{C}_{\text{cc}}$ and
144 Sr isotopes.



145 Calcite isotopes were measured using a ThermoFisher Delta^{plus}XL isotope ratio mass spectrometer
146 (IRMS) equipped with a Gasbench II interface at the University of Innsbruck, according to standard
147 methods (Spötl, 2011). Fluid inclusions were examined in doubly-polished thick section (100 µm)
148 slides, using a Nikon Eclipse E400 POL microscope. The isotope composition of fluid inclusion water
149 was measured at the University of Innsbruck using a Delta V Advantage IRMS coupled to a Thermal
150 Combustion/Elemental Analyser and a ConFlow II interface (Thermo Fisher) using the line, crusher
151 and cryo-focussing cell described in Dublyansky and Spötl (2009). Samples were cut with a diamond
152 band saw along visible petrographic boundaries in the speleothem, and therefore represent specific
153 growth increments. Samples were analysed at least in duplicate, with the standard sampling protocol
154 used on the Innsbruck instrument (Dublyansky and Spötl, 2009). To exclude the possibility of post-
155 depositional diagenetic alteration, petrographic thin sections were investigated using transmitted-light
156 microscopy. Results are detailed in Supplemental Information 1.

157 Optical emission spectroscopy (OES) was used to measure a variety of elemental concentrations,
158 including Sr, along the main growth axis of SC-06-01. The low spatial resolution of trace elemental
159 analyses (every 10 mm) does not allow to investigate time series of elemental variation but was useful
160 to assess Sr contents of the samples for Sr isotope measurements by thermal ionisation mass
161 spectrometry (TIMS). The samples for TIMS analyses were drilled using a hand held micro drill with
162 a tungsten carbide drill bit. Sample sizes range between 2 and 4 mg, thus we achieved a minimum Sr
163 load of 100 ng on the Re filaments for TIMS. Chemical sample preparation and subsequent TIMS
164 measurement were done following standard protocols (Charlier et al., 2006). No spike was added to
165 the samples prior to chemical purification. The Sr isotope measurements were done on a Triton TIMS
166 housed at the Bristol Isotope Group laboratory, University of Bristol.



167 Results

168 **Fluid inclusions**

169 Petrographic analysis of the thick sections indicates that the distribution of fluid inclusions is highly
170 variable, with macroscopically opaque “milky” calcite typical of rapidly growing intervals containing
171 sometimes very abundant inclusions and the discoloured, translucent calcite of the slowly growing
172 intervals being almost inclusion-free (Fig. 2). In most samples, two distinct populations of inclusions
173 were identified with numerous small intra-crystalline inclusions and larger, but less frequent, inter-
174 crystalline inclusions. Consequently, the volume of water analysed per sample was very variable (Fig.
175 3). Indeed, a significant proportion of individual fluid inclusion measurements had analyte volumes
176 too small ($<0.1 \mu\text{L}$) to have confidence in the isotope results. A small number of analyses failed due
177 to excessive water saturating the detector, and these have not been included in the datasets presented
178 here. The major impact of the highly variable availability of inclusions in the speleothem is a
179 significant bias in the analyses towards the most rapidly growing, and therefore probably humid, time
180 periods.

181 In most samples, achieving within-error replication ($\delta^2\text{H} \pm 1.5\text{‰}$, $\delta^{18}\text{O}: \pm 0.5\text{‰}$) of both $\delta^{18}\text{O}_{\text{fi}}$ and
182 $\delta^2\text{H}_{\text{fi}}$ was difficult. This must reflect more than one population of inclusions with different properties
183 being present within at least some samples, and each replicate analysis represents some proportion of
184 mixing between these populations. This suggests significant short-term variability in the composition
185 of the water stored in the presumably rather small soil/epikarst zone overlying the cave.

186 Consequently, any given time interval risks being under-sampled with regard to variability at that
187 time. Although there is some visual correspondence between the $\delta^{18}\text{O}_{\text{fi}}$, $\delta^2\text{H}_{\text{fi}}$ and $\delta^{18}\text{O}_{\text{cc}}$ data series
188 (Fig. 4), the usefulness of interpretation that can be drawn from the episodic SC-01-06 fluid inclusion
189 dataset when arranged as a time series is limited. We therefore largely limit our discussion to the
190 properties of the population of waters as a full dataset.

191 Figure 5 shows the SC-06-01 fluid inclusion dataset alongside Global Natural Isotopes in
192 Precipitation (GNIP) datasets from Tunis World Meteorological Office (WMO station 6071500), Sfax



193 (6075000) and Bet Dagan (4017900) (locations in Fig. 1) and other published precipitation datasets.
194 The Tunisian datasets fit within a trend typical of the Global Meteoric Water Line (GMWL) ($\delta^2\text{H} =$
195 $8\delta^{18}\text{O} + 10$). However, all this data lies along a single moisture evolution trend, and the Tunis and
196 Sfax populations overlap. The data from Bet Dagan exhibits a trend which is extremely close to being
197 parallel to the global trend dominating in Tunisia, but translated by +10 ‰ in $\delta^2\text{H}$, reflecting greater
198 deuterium excess. This is typical of the Mediterranean Meteoric Water Line (MMWL) (Ayalon et al.,
199 1998; Gat et al., 2003), and reflects internal recycling of water with consequent deuterium enrichment
200 in the eastern Mediterranean and its bordering continental areas.

201 The values of $\delta^2\text{H}_{\text{fi}}$ and $\delta^{18}\text{O}_{\text{fi}}$ fit within the range of values for modern precipitation, giving
202 confidence that these measurements do reflect past precipitation composition despite the influence of
203 multiple inclusion populations. The lack of apparent scatter towards positive $\delta^{18}\text{O}$ values both in the
204 precipitation and fluid inclusion datasets further indicates that the data represent little-altered
205 precipitation values, and that surface re-evaporation was minor at least during humid phases.
206 However, the range of fluid inclusion values is inconsistent with either an exclusively Tunis-type or
207 an exclusively Bet Dagan-type moisture source for precipitation in Cyrenaica during MIS 3. Even
208 when all but the subset of fluid inclusion analyses who replicates are similar are excluded (Fig. 6), the
209 population is split between the Tunisian and Israeli precipitation end-members.

210

211 **Strontium isotopes**

212 The $^{87}\text{Sr}/^{86}\text{Sr}$ signal in the SC-06-01 record is rather invariable (Fig. 7), with all analyses indicating
213 values within analytical error. Mean values vary between 0.708275 and 0.708524 and although there
214 is an apparent trend from maxima at 34 and 64 ka BP with a minimum at 52 ka BP, which mimics the
215 precession history, this is too weak to be significant relative to the error.

216 **Calcite carbon isotopes**

217 Both $\delta^{13}\text{C}_{\text{cc}}$ and $\delta^{18}\text{O}_{\text{cc}}$ show similar trends throughout the record (Fig. 8), indicating that depleted
218 oxygen isotopes coincide with depleted carbon isotope values. This does not appear to arise from



219 fractionation on the speleothem surface (Hoffmann et al., 2016), and so represents changes in soil
220 bioproductivity acting in concert with changes in precipitation.

221 Discussion

222 Moisture advection during Libyan humid phases

223 The range of values of both individual and replicated fluid inclusion measurements can only be
224 reconciled with multiple moisture sources. Most of the fluid inclusion data cluster between the
225 weighted mean value for precipitation collected at Sfax with a mixed source from the Atlantic and
226 western Mediterranean, (“Sfax Mixed” $\delta^{18}\text{O}_{\text{ppt}} = -4.93 \text{ ‰}$, $\delta^2\text{H}_{\text{ppt}} = -26 \text{ ‰}$; Fig. 9) and High
227 Precipitation events at Bet Dagan ($\delta^{18}\text{O}_{\text{ppt}} = -6.33 \text{ ‰}$, $\delta^2\text{H}_{\text{ppt}} = -21.46 \text{ ‰}$; Fig. 9). This value is
228 representative of many of the largest individual precipitation events at Sfax in the period 1992-1999
229 associated with a Western Mediterranean moisture source (Celle-Jeanton et al., 2001). However, the
230 fluid inclusion data cluster also extends to the end member reflecting pure western Mediterranean
231 sources at Sfax ($\delta^{18}\text{O}_{\text{ppt}} = -3.99 \text{ ‰}$, $\delta^2\text{H}_{\text{ppt}} = -20.3 \text{ ‰}$; Fig. 9), indicating a third end member
232 composition with higher $\delta^{18}\text{O}_{\text{ppt}}$. Consequently, we consider that this data reflects a dynamic balance
233 of moisture sources contributing to rainfall in Cyrenaica which resembles modern precipitation in
234 Tunisia and Israel in roughly equal proportions.

235 The weighted mean value for Atlantic-sourced precipitation events in Sfax ($\delta^{18}\text{O}_{\text{ppt}} = -6.7 \text{ ‰}$, $\delta^2\text{H}_{\text{ppt}} =$
236 -37.7 ‰) is distant from any observed fluid inclusion value (Fig. 9). Likewise, compositions similar to
237 the high amount Atlantic-sourced rainfall events in Sfax ($\delta^{18}\text{O}_{\text{ppt}} = -8 \text{ ‰}$, $\delta^2\text{H}_{\text{ppt}} = -46 \text{ ‰}$) are not
238 reflected in the fluid inclusion data in Figure 9 suggesting a relatively low admixture of water from
239 this source. A simple 3-end-member unmixing of fluid inclusion isotope values using the quantitative
240 approach of (Rogerson et al., 2011) indicates that Atlantic-sourced water supplied no more than 15 %
241 of the mass for any given fluid inclusion analysis. However, the coherence of fluid inclusion isotope
242 ratios with the weighted mean of “mixed” Atlantic and Mediterranean precipitation at Sfax suggests
243 that this small Atlantic influence is nevertheless persistent, and this must reflect synoptic westerly
244 storms (Celle-Jeanton et al., 2001). An alternative way to explain the trend of some points towards



245 enriched $\delta^{18}\text{O}$ values on the GMWL would be the temperature-dependent fractionation that would be
246 caused by a shift to summertime precipitation. We do not favour this explanation as it requires a more
247 fundamental reorganisation of regional atmospheric circulation than our suggestion that the winter
248 storms observed today penetrated further east in the past.

249 Within the data presented in Figure 9, the Phase II fluid inclusions are exceptional, because none
250 show compositions consistent with a Bet Dagan source. Indeed, all the measurements for this period
251 resemble GMWL compositions. This seems to reflect a fundamental difference between this period
252 and Phases I and III, where all precipitation is drawn from synoptic westerly storms in the winter.
253 Consequently, it would seem that during the Obliquity-forced period of humidity the Israeli-mode
254 precipitation did not occur in the manner that it did during both Precession-forced periods of
255 humidity.

256 Although the isotopic composition of Mediterranean water will have been more enriched during MIS
257 3 due to ice-volume effects and increased Mediterranean water residence time (Rohling and Bryden,
258 1994), the similar mean values of the SC-06-01 fluid inclusion waters compared to modern
259 precipitation indicates the meteoric waterline at this time was not displaced to more enriched isotope
260 values. This could reflect balancing of source water effects by changes in kinetic fractionation during
261 evaporation (Goldsmith et al., 2017), which is controlled by normalised relative humidity. This would
262 imply that the Mediterranean air masses were less saturated with moisture than today during MIS 3,
263 which is consistent with the high deuterium excess $\delta^2\text{H}_{\text{excess}}$ values found in some fluid inclusion
264 samples (Fig. 10), but is difficult to reconcile with the increased precipitation recorded in SC-06-01.
265 Alternatively, the source water effect may be countered by increased runoff from the margins of the
266 Mediterranean supplying isotopically depleted water to evaporating surface water. Isotopic
267 “residuals” consistent with this argument are identified throughout MIS 3 in the eastern
268 Mediterranean marine core LC21 (Grant et al., 2016), and this is also consistent with higher rainfall in
269 Cyrenaica. We therefore favour the latter explanation.

270 We conclude that most of the precipitation supplied to Cyrenaica during MIS 3 was sourced from
271 within the Mediterranean basin, which exhibited a similar meteoric water cycle to that observed today



272 albeit with more freshwater influence. This is a critical observation, as internally-cycled water cannot
273 alter the basin-scale hydrological balance and therefore is a minor influence on deep convection in the
274 Mediterranean Sea (Bethoux and Gentili, 1999). The precipitation feeding runoff must be externally
275 sourced if it is to materially change Mediterranean functioning, as is observed during sapropel events
276 (Rohling et al., 2015). As most of the precipitation identified in SC-06-01 is sourced internally to the
277 Mediterranean, only the small, Atlantic-sourced portion of this water can be assumed to play a role in
278 Mediterranean freshening. This conclusion is likely transferable to any site on the continental margins
279 of the Mediterranean. This observation is critical, as it decouples the processes of precipitation on the
280 Mediterranean margins with sapropel formation, and consequent changes in momentum transfer to the
281 North Atlantic (Rogerson et al., 2012). Consequently, we recommend that great care is taken to
282 determine whether past precipitation peaks reflect significantly enhanced external water advection
283 before any continental record can be used as a basis for inferring Mediterranean freshening.

284 **Palaeoclimatological significance**

285 The consistency of MIS 3 and modern precipitation isotope values permits comparison of fluid
286 inclusion values and precipitation magnitude records at Sfax and Bet Dagan. Most of the water
287 reaching Susah Cave seems to have been derived from large-magnitude rainfall sourced from the
288 Western or Eastern Mediterranean surface water. The primary difference between these end-members
289 is the level of D_{excess} , with the Western water $\sim 10\%$ and Eastern water $\sim 30\%$. This difference allows
290 the influence of these two sources to be compared between the three major humid phases (Hoffmann
291 et al., 2016) recorded in SC-06-01 (Fig. 10). These phases reflect changes in the distribution of
292 insolation as a consequence of changes in orbital tilt, with Phase I (65 to 61 ka BP) and Phase III
293 (37.5 to 33.5 ka BP) associated with reflecting Northern Hemisphere heating during precession
294 minima and Phase II (52.5 to 50.5 ka BP) which has been associated with a change in obliquity. In all
295 cases, the peak in rainfall recorded by the speleothem leads the orbital peak by ~ 3 ka. Phases I and III
296 both show very elevated D_{excess} , whereas no such values were found in Phase II. This provides further
297 support to our conclusion that the Eastern Mediterranean source contributed significant moisture to
298 Cyrenaica during precession-related humid events, but that it did not during the obliquity-related



299 humid event. This difference in the origin of the moisture feeding rainfall may explain the difference
300 in average $\delta^{18}\text{O}_{\text{cc}}$ during these different phases (Hoffmann et al., 2016).

301 The varying balance between Eastern and Western precipitation is diagnostic of changing basin-scale
302 atmospheric structure during the past. Eastern-sourced rainfall may occasionally relate to wintertime
303 storms, as today (Gat et al., 2003), but essentially reflects convective rainfall with relatively small
304 advection distances. The significant enhancement of the magnitude and regional significance of this
305 convective rainfall observed at Susah Cave must reflect greater atmospheric convergence due to
306 northward displacement of the annual average position of the ITCZ (Tuenter et al., 2003). Contrary to
307 this, the Western-sourced moisture is transported ~1500 km eastwards to reach Cyrenaica, which must
308 reflect the mid-latitude storm track (Brayshaw et al., 2009). Consequently, although it does not seem
309 that Atlantic moisture is important to the climatology of Cyrenaica, the momentum derived from
310 Atlantic winter storms predicted by regional climate modelling (Brayshaw et al., 2009) and observed
311 on the northern Mediterranean margin (Toucanne et al., 2015) remains pivotal to supplying moisture
312 to North Africa. Within obliquity-forced phases, advective transport of moisture alone drives
313 humidity. In contrast, we conclude that during precession-forced humid phases, the impact of
314 advective transport of moisture from the Western to the Eastern Mediterranean basin occurs alongside
315 strong convergence and convective rainfall within the eastern basin. The dilution of the advective
316 signal by internal convective rainfall may be the reason why Dansgaard-Oeschger cycles in the North
317 Atlantic are well reflected at Susah Cave during high precession (Hoffmann et al., 2016), whereas
318 there is weaker correspondence of Cyrenaican rain and North Atlantic heat during low precession.

319 Further constraint on large-scale atmospheric advection can be provided by Sr-isotopes, which are
320 known to be sensitive to changes in transport of Saharan dust (Frumkin and Stein, 2004). Even
321 considering the most slow-growing and most rapidly-growing parts of SC-06-01, no significant
322 difference in $^{87}\text{Sr}/^{86}\text{Sr}$ was identified. This is unexpected and significant, as climate-driven changes in
323 $^{87}\text{Sr}/^{86}\text{Sr}$ have previously been reported from speleothems in the Mediterranean region (Frumkin and
324 Stein, 2004). It seems that despite changes in the intensity of moisture transport during the period 65-
325 30 ka BP, there is no large-scale change in atmospheric dust transport direction. This further supports



326 our conclusion from the fluid inclusions that the Eastern Mediterranean rainfall operating during
327 precession minima reflects enhanced internal convection rather than transport of moisture from the
328 east or south with an atmospheric circulation pattern that prevails today.

329 *Implications for Susah Cave $\delta^{18}O_{cc}$*

330 Aside from those data with high deuterium excess, which reflect influence from the Eastern
331 Mediterranean source, much of the variance in the fluid inclusion dataset is captured by a two end-
332 member mixing system resembling modern rainfall in Tunisia. One end-member is the Western
333 Mediterranean source of Celle-Jeanton et al (2003), but the other is isotopically too heavy to be
334 identified with the Atlantic source. Rather, it resembles the “Sfax Mixed” population defined by
335 Celle-Jeanton et al (2003), reflecting a mixed source of moisture from both the Western
336 Mediterranean and Atlantic. Consequently, although quantitatively minor amounts of Atlantic water
337 reached the site, changes in the moisture advection driven by westerly winds had a strong influence on
338 $\delta^{18}O_{dripwater}$ trends in time. At Sfax today, this influence causes a prominent bimodal behaviour with
339 two rainfall maxima with different $\delta^{18}O_{ppt}$, which eliminates a simple and quantitative rainfall amount
340 control on precipitation, which can be observed at Tunis (WMO code 6071500,
341 <https://nucleus.iaea.org/wiser/gnip.php>). Furthermore, addition of heavy rain events derived from the
342 Eastern Mediterranean aliases the tendency towards depleted $\delta^{18}O_{dripwater}$, as this water is also more
343 depleted than modern Western Mediterranean precipitation. In the Bet Dagan data, there is also a
344 tendency to lower $\delta^{18}O_{ppt}$ with higher precipitation amount, but the relationship between rainfall
345 amount and rainfall isotope composition is not identical to Tunis. Ultimately, it seems likely that
346 rainfall amount changes at Susah Cave do cause depleted (enriched) $\delta^{18}O_{cc}$ values to be associated
347 with high (low) rainfall, but this is too complicated by independent changes increases (decreases) in
348 westerly moisture advection and increases (decreases) in convergence. Qualitatively, all these
349 parameters are expected symptoms of North African humid phases and so these trends remain a
350 valuable expression of climatic variability. Quantitatively, more information is required to translate
351 the trends into fully-functional palaeoclimatologies, and this analysis pivots on whether $\delta^{18}O_{cc}$ trends
352 reflect changes in water deficit / surplus in Cyrenaica.



353 Although it is likely the oxygen isotope fractionation during calcite precipitation occurred close to
354 isotope equilibrium (Hoffmann et al., 2016), there is a good degree of correspondence between
355 positive and negative phases in $\delta^{18}\text{O}_{\text{cc}}$ and $\delta^{13}\text{C}_{\text{cc}}$, indicating a shared control. Indeed, $\delta^{13}\text{C}_{\text{cc}}$ has a
356 markedly higher amplitude variability than $\delta^{18}\text{O}_{\text{cc}}$. More isotopically depleted carbon may represent
357 increased incorporation of respired soil carbon, increased dominance of C3 over C4 plants, and/or
358 decreased degassing of aquifer water (Baker et al., 1997). Today, the Susah Cave location on Jebel
359 Malh has very thin soil cover, colonised by shrubby maquis vegetation. Soil respiration and
360 colonisation by C3 plants is limited by the strong water deficit of the region, and aquifer water
361 outgassing is enhanced by long residence times due to low water infiltration. Increased water
362 availability will progressively deplete the $\delta^{13}\text{C}$ of dripwater by all three mechanisms described above.
363 Consequently, all three of these processes promote correlation between $\delta^{13}\text{C}_{\text{cc}}$ and precipitation
364 amount. Within the $\delta^{18}\text{O}_{\text{cc}}$ data series, peak growth rates occur both during relatively enriched and
365 relatively depleted isotope stages. This is not the case for $\delta^{13}\text{C}_{\text{cc}}$, which more consistently shows
366 depleted values during times of rapid growth (SC-06-01 growth phases shown in Fig. 11). We
367 therefore consider it likely that $\delta^{13}\text{C}_{\text{cc}}$ indeed more accurately records rainfall amount than $\delta^{18}\text{O}_{\text{cc}}$ does.

368 Conclusions and Implications

369 A key feature of this combined dataset is the long-term sinusoidal trend in both the $\delta^{18}\text{O}_{\text{cc}}$ and $\delta^2\text{H}_{\text{fi}}$,
370 reflecting the differing rainfall regimes dominant between Humid Phases I and III compared to Phase
371 II. This is not developed in $\delta^{13}\text{C}_{\text{cc}}$, implying that the process forcing the long-term cycle in moisture
372 source is not impacting on carbon dynamics in the soil and epikarst. We therefore conclude that there
373 is a mixed amount and source control on $\delta^{18}\text{O}$ and $\delta^2\text{H}$ in the SC-01-06 record, whereas $\delta^{13}\text{C}$ is
374 dominantly controlled by water availability.

375 The fluid inclusions from SC-06-01 show that rainfall compositions in the southeast Mediterranean
376 region during MIS 3 were comparable to modern rainfall compositions recorded in regional GNIP
377 datasets. However, the diversity of compositions is impossible to explain with a single rainfall source,
378 rather indicating that moisture derived from the Atlantic, the Western Mediterranean and the Eastern



379 Mediterranean basins have all contributed to MIS 3 precipitation in Libya. This requires both
380 enhanced westerly advection of moisture to this region, reflecting the Atlantic storm track, and
381 enhanced convective rainfall within the Eastern Mediterranean basin. There is some indication that
382 these two mechanisms differ in terms of their response to orbital forcing, with precession minima
383 enhancing westerly advection and internal convection, whereas obliquity minima enhance westerly
384 advection without significantly altering internal convection.

385 Crucially, this picture is most consistent with atmospheric circulation over the Mediterranean
386 remaining essentially unchanged during precession cycles. This is consistent with regional climate
387 model experiments showing major enhancement of winter westerly storm activity, but it not
388 consistent with the extreme migration of the ITCZ, where the monsoon belt approaches the North
389 African coast. The strong implication is that a significant arid belt is retained between the
390 Mediterranean and the ITCZ, even when northernmost Africa is experiencing significantly enhanced
391 rainfall.

392 It is likely that rainfall amount played a role in controlling the isotopic composition of the calcite in
393 this speleothem ($\delta^{18}\text{O}_{\text{cc}}$). However, the more depleted values reflecting higher rainfall are also
394 consistent with different mixing between the end members identified by the fluid inclusion analysis.
395 The structure of the $\delta^{13}\text{C}_{\text{cc}}$ record provides an independent means of assessing changes in water
396 surplus / deficit, as more depleted values will reflect lower aquifer residence times, enhanced soil
397 respiration and changes in vegetation structure, all of which are limited by water availability in this
398 semi-arid environment. Combined analysis of the proxies provides a powerful new demonstration that
399 the northeast Libyan climate was more humid during millennial-scale warm periods in the North
400 Atlantic realm, but quantification will be dependent on generating unambiguous independent evidence
401 for water availability in the soil and epikarst.

402 Acknowledgements

403 We thank the Royal Geographical Society for the pump-priming investment that began this work
404 (Thesiger-Oman International Fellowship 2009), the Natural Environment Research Council for



405 providing the funds that made the analytical work on this project possible (NE/J014133/1) and The
406 Leverhulme Trust for funding activities within the associated International Network (IN-2012-113).

407 References

- 408 Arienzo, M.M. et al. 2015. Bahamian speleothem reveals temperature decrease associated with
409 Heinrich stadials. *EPSL* 430, 377-386.
- 410 Adkins, J., Demenocal, P., and Eshel, G.: The “African humid period” and the record of marine
411 upwelling from excess 230Th in Ocean Drilling Program Hole 658C, *Paleoceanography and*
412 *Paleoclimatology*, 21, 2006.
- 413 Ait Brahim, Y., Cheng, H., Sifeddine, A., Wassenburg, J. A., Cruz, F. W., Khodri, M., Sha, L., Pérez-
414 Zanón, N., Beraaouz, E. H., Apaéstegui, J., Guyot, J.-L., Jochum, K. P., and Bouchaou, L.: Speleothem
415 records decadal to multidecadal hydroclimate variations in southwestern Morocco during the last
416 millennium, *Earth and Planetary Science Letters*, 476, 1-10,
417 <https://doi.org/10.1016/j.epsl.2017.07.045>, 2017.
- 418 Arienzo, M. M., Swart, P. K., Pourmand, A., Broad, K., Clement, A. C., Murphy, L. N., Vonhof, H. B.,
419 and Kakuk, B.: Bahamian speleothem reveals temperature decrease associated with Heinrich
420 stadials, *Earth and Planetary Science Letters*, 430, 377-386, 2015.
- 421 Armitage, S. J., Drake, N. A., Stokes, S., El-Hawat, A., Salem, M., White, K., Turner, P., and McLaren, S.
422 J.: Multiple phases of north African humidity recorded in lacustrine sediments from the fazzan basin,
423 Libyan sahara, *Quaternary Geochronology*, 2, 181-186, 2007.
- 424 Ayalon, A., Bar-Matthews, M., and Sass, E.: Rainfall-recharge relationships within a karstic terrain in
425 the Eastern Mediterranean semi-arid region, Israel: $\delta^{18}\text{O}$ and δD characteristics, *Journal of*
426 *Hydrology*, 207, 18-31, [10.1016/S0022-1694\(98\)00119-X](https://doi.org/10.1016/S0022-1694(98)00119-X), 1998.
- 427 Baker, A., Ito, E., Smart, P. L., and McEwan, R. F.: Elevated and variable values of ^{13}C in speleothems
428 in a British cave system, *Chemical Geology*, 136, 263-270, 1997.
- 429 Ballais, J.-L.: Evolution holocène de la Tunisie saharienne et présaharienne, *Méditerranée*, 74, 31-38,
430 1991.
- 431 Bethoux, J. P., and Gentili, B.: Functioning of the Mediterranean Sea: past and present changes
432 related to freshwater input and climate changes, *Journal of Marine Systems*, 20, 33-47, 1999.
- 433 Black, E., Brayshaw, D. J., and Rambeau, C. M. C.: Past, present and future precipitation in the Middle
434 East: Insights from models and observations, *Philosophical Transactions of the Royal Society A:*
435 *Mathematical, Physical and Engineering Sciences*, 368, 5173-5184, [10.1098/rsta.2010.0199](https://doi.org/10.1098/rsta.2010.0199), 2010.
- 436 Bosmans, J. H. C., Drijfhout, S. S., Tuenter, E., Hilgen, F. J., Lourens, L. J., and Rohling, E. J.: Precession
437 and obliquity forcing of the freshwater budget over the Mediterranean, *Quaternary Science*
438 *Reviews*, 123, 16-30, [10.1016/j.quascirev.2015.06.008](https://doi.org/10.1016/j.quascirev.2015.06.008), 2015.
- 439 Brayshaw, D. J., Woollings, T., and Vellinga, M.: Tropical and Extratropical Responses of the North
440 Atlantic Atmospheric Circulation to a Sustained Weakening of the MOC, *Journal of Climate*, 22, 3146-
441 3155, [10.1175/2008jcli2594.1](https://doi.org/10.1175/2008jcli2594.1), 2009.
- 442 Celle-Jeanton, H., Zouari, K., Travi, Y., and Daoud, A.: Caractérisation isotopique des pluies en
443 Tunisie. Essai de typologie dans la région de Sfax, *Sciences de la Terre et des planètes*, 333, 625-631,
444 2001.
- 445 Charlier, B., Ginibre, C., Morgan, D., Nowell, G., Pearson, D., Davidson, J., and Ottley, C.: Methods for
446 the microsampling and high-precision analysis of strontium and rubidium isotopes at single crystal
447 scale for petrological and geochronological applications, *Chemical Geology*, 232, 114-133, 2006.
- 448 Collins, J. A., Prange, M., Caley, T., Gimeno, L., Beckmann, B., Mulitza, S., Skonieczny, C., Roche, D.,
449 and Schefuß, E.: Rapid termination of the African humid period triggered by northern high-latitude
450 cooling, *Nature Communications*, 8, 1372, 2017.



- 451 deMenocal, P., Ortiz, J., Guilderson, T., Adkins, J., Sarnthein, M., Baker, L., and Yarusinsky, M.: Abrupt
452 onset and termination of the African Humid Period: rapid climate responses to gradual insolation
453 forcing, *Quaternary Science Reviews*, 19, 347- 361, 2000.
- 454 Drake, N. A., El-Hawat, A. S., Turner, P., Armitage, S. J., Salem, M. J., White, K. H., and McLaren, S.:
455 Palaeohydrology of the Fazzan Basin and surrounding regions: The last 7 million years,
456 *Palaeogeography Palaeoclimatology Palaeoecology*, 263, 131-145, [10.1016/j.palaeo.2008.02.005](https://doi.org/10.1016/j.palaeo.2008.02.005),
457 2008.
- 458 Drake, N. A., Blench, R. M., Armitage, S. J., Bristow, C. S., and White, K. H.: Ancient watercourses and
459 biogeography of the Sahara explain the peopling of the desert, *Proc. Natl. Acad. Sci. U. S. A.*, 108,
460 458-462, [10.1073/pnas.1012231108](https://doi.org/10.1073/pnas.1012231108), 2011.
- 461 Dublyansky, Y. V., and Spötl, C.: Hydrogen and oxygen isotopes of water from inclusions in minerals:
462 Design of a new crushing system and on-line continuous-flow isotope ratio mass spectrometric
463 analysis, *Rapid Communications in Mass Spectrometry*, 23, 2605-2613, [10.1002/rcm.4155](https://doi.org/10.1002/rcm.4155), 2009.
- 464 Fleitmann, D., Burns, S. J., Neff, U., Mangini, A., and Matter, A.: Changing moisture sources over the
465 last 330,000 years in Northern Oman from fluid-inclusion evidence in speleothems, *Quaternary*
466 *Research*, 60, 223-232, [http://dx.doi.org/10.1016/S0033-5894\(03\)00086-3](https://doi.org/10.1016/S0033-5894(03)00086-3), 2003.
- 467 Fontes, J. C., and Gasse, F.: PALHYDAF (Palaeohydrology in Africa) program: objectives, methods,
468 major results, *Palaeogeography, Palaeoclimatology, Palaeoecology*, 84, 191-215, [10.1016/0031-
469 0182\(91\)90044-R](https://doi.org/10.1016/0031-0182(91)90044-R), 1991.
- 470 Frumkin, A., and Stein, M.: The Sahara-East Mediterranean dust and climate connection revealed by
471 strontium and uranium isotopes in a Jerusalem speleothem, *Earth and Planetary Science Letters*,
472 217, 451-464, [10.1016/S0012-821X\(03\)00589-2](https://doi.org/10.1016/S0012-821X(03)00589-2), 2004.
- 473 Gasse, F., and Campo, E. v.: Abrupt post-glacial climate events in west Asia and north Africa
474 monsoon domains, *Earth and Planetary Science Letters*, 126, 435-456, 1994.
- 475 Gasse, F.: Diatom-inferred salinity and carbonate oxygen isotopes in Holocene waterbodies of the
476 western Sahara and Sahel (Africa), *Quaternary Science Reviews*, 21, 737-767, 2002.
- 477 Gat, J. R., Klein, B., Kushnir, Y., Roether, W., Wernli, H., Yam, R., and Shemesh, A.: Isotope
478 composition of air moisture over the Mediterranean Sea: An index of the air-sea interaction pattern,
479 *Tellus, Series B: Chemical and Physical Meteorology*, 55, 953-965, [10.1034/j.1600-
480 0889.2003.00081.x](https://doi.org/10.1034/j.1600-0889.2003.00081.x), 2003.
- 481 Genty, D., Blamart, D., Ghaleb, B., Plagnes, V., Causse, C., Bakalowicz, M., Zouari, K., Chkir, N.,
482 Hellstrom, J., Wainer, K., and Bourges, F.: Timing and dynamics of the last deglaciation from
483 European and North African $\delta^{13}\text{C}$ stalagmite profiles-comparison with Chinese and South
484 Hemisphere stalagmites, *Quaternary Science Reviews*, 25, 2118-2142, 2006.
- 485 Goldsmith, Y., Polissar, P. J., Ayalon, A., Bar-Matthews, M., deMenocal, P. B., and Broecker, W. S.:
486 The modern and Last Glacial Maximum hydrological cycles of the Eastern Mediterranean and the
487 Levant from a water isotope perspective, *Earth and Planetary Science Letters*, 457, 302-312,
488 [http://dx.doi.org/10.1016/j.epsl.2016.10.017](https://doi.org/10.1016/j.epsl.2016.10.017), 2017.
- 489 Grant, K. M., Grimm, R., Mikolajewicz, U., Marino, G., Ziegler, M., and Rohling, E. J.: The timing of
490 Mediterranean sapropel deposition relative to insolation, sea-level and African monsoon changes,
491 *Quaternary Science Reviews*, 140, 125-141, [http://dx.doi.org/10.1016/j.quascirev.2016.03.026](https://doi.org/10.1016/j.quascirev.2016.03.026),
492 2016.
- 493 Harrison, S., Bartlein, P., Izumi, K., Li, G., Annan, J., Hargreaves, J., Braconnot, P., and Kageyama, M.:
494 Evaluation of CMIP5 palaeo-simulations to improve climate projections, *Nature Climate Change*, 5,
495 735-743, 2015.
- 496 Hoffmann, D. L., Rogerson, M., Spötl, C., Luetscher, M., Vance, D., Osborne, A. H., Fello, N. M., and
497 Moseley, G. E.: Timing and causes of North African wet phases during MIS 3 and implications for
498 Modern Human migration, *Nature Scientific Reports*, 6, 36367, 2016.
- 499 IPCC: Climate Change 2014: Impacts, Adaptation, and Vulnerability. Part B: Regional Aspects.
500 Contribution of Working Group II to the Fifth Assessment Report of the Intergovernmental Panel on
501 Climate Change, United Kingdom and New York, 688, 2014.



- 502 Jolly, D., Prentice, I. C., Bonnefille, R., Ballouche, A., Bengo, M., Brenac, P., Buchet, G., Burney, D.,
503 Cazet, J. P., Cheddadi, R., Edorh, T., Elenga, H., Elmoutaki, S., Guiot, J., Laarif, F., Lamb, H., Lezine, A.
504 M., Maley, J., Mbenza, M., Peyron, O., Reille, M., Reynaud-Farrera, I., Riollet, G., Ritchie, J. C., Roche,
505 E., Scott, L., Ssemmanda, I., Straka, H., Umer, M., Van Campo, E., Vilimumbalo, S., Vincens, A., and
506 Waller, M.: Biome reconstruction from pollen and plant macrofossil data for Africa and the Arabian
507 peninsula at 0 and 6000 years, *Journal of Biogeography*, 25, 1007-1027, 1998.
- 508 McGarry, S., Bar-Matthews, M., Matthews, A., Vaks, A., Schilman, B., and Ayalon, A.: Constraints on
509 hydrological and paleotemperature variations in the Eastern Mediterranean region in the last 140 ka
510 given by the δD values of speleothem fluid inclusions, *Quaternary Science Reviews*, 23, 919-934,
511 <http://dx.doi.org/10.1016/j.quascirev.2003.06.020>, 2004.
- 512 Meckler, A. N., Affolter, S., Dublyansky, Y. V., Krüger, Y., Vogel, N., Bernasconi, S. M., Frenz, M.,
513 Kipfer, R., Leuenberger, M., Spötl, C., Carolin, S., Cobb, K. M., Moerman, J., Adkins, J. F., and
514 Fleitmann, D.: Glacial–interglacial temperature change in the tropical West Pacific: A comparison of
515 stalagmite-based paleo-thermometers, *Quaternary Science Reviews*, 127, 90-116,
516 <http://dx.doi.org/10.1016/j.quascirev.2015.06.015>, 2015.
- 517 Osborne, A., Vance, D., Rohling, E., Barton, N., Rogerson, M., and Fello, N.: A humid corridor across
518 the Sahara for the migration of early modern humans out of Africa 120,000 years ago, *Proc. Natl.*
519 *Acad. Sci. U. S. A.*, doi_10.1073_pnas.0804472105, 2008.
- 520 Osborne, A. H., Marino, G., Vance, D., and Rohling, E. J.: Eastern Mediterranean surface water Nd
521 during Eemian sapropel S5: monitoring northerly (mid-latitude) versus southerly (sub-tropical)
522 freshwater contributions, *Quaternary Science Reviews*, 29, 2473-2483,
523 <http://dx.doi.org/10.1016/j.quascirev.2010.05.015>, 2010.
- 524 Pascale, S., Gregory, J. M., Ambaum, M., and Tailleux, R.: Climate entropy budget of the HadCM3
525 atmosphere-ocean general circulation model and of FAMOUS, its low-resolution version, *Climate*
526 *Dynamics*, 36, 1189-1206, 10.1007/s00382-009-0718-1, 2011.
- 527 PETIT-MAIRE, N., BUROLLET, P. F., A BALLAIS, J.-L., A FONTUGNE, M., A ROSSO, J.-C., A LAZAAR, A.,
528 and Gauthier-Villars, I.: Paléoclimats holocènes du Sahara septentrional. Dépôts lacustres et
529 terrasses alluviales en bordure du Grand Erg Oriental à l'extrême-Sud de la Tunisie, *Comptes rendus*
530 *de l'Académie des sciences. Série 2, Mécanique, Physique, Chimie, Sciences de l'univers, Sciences de*
531 *la Terre* 312, 1661-1666, 1991.
- 532 Peyron, O., Jolly, D., Braconnot, P., Bonnefille, R., Guiot, J., Wirmann, D., and Chalie, F.: Quantitative
533 reconstructions of annual rainfall in Africa 6000 years ago: Model-data comparison, *Journal of*
534 *Geophysical Research-Atmospheres*, 111, D24110
535 Artn d24110, 2006.
- 536 Prentice, I. C., and Jolly, D.: Mid-Holocene and glacial-maximum vegetation geography of the
537 northern continents and Africa, *Journal of Biogeography*, 27, 507-519, 2000.
- 538 Rogerson, M., Schönfeld, J., and Leng, M.: Qualitative and quantitative approaches in
539 palaeohydrography: A case study from core-top parameters in the Gulf of Cadiz, *Marine Geology*,
540 280, 150-167, 2011.
- 541 Rogerson, M., Rohling, E. J., Bigg, G. R., and Ramirez, J.: Palaeoceanography of the Atlantic-
542 Mediterranean Exchange: Overview and first quantitative assessment of climatic forcing, *Reviews*
543 *of Geophysics*, 50, DOI: 8755-1209/8712/2011RG000376, 2012.
- 544 Rohling, E., Marino, G., and Grant, K.: Mediterranean climate and oceanography, and the periodic
545 development of anoxic events (sapropels), *Earth-Science Reviews*, 143, 62-97, 2015.
- 546 Rohling, E. J., and Bryden, H. L.: Estimating past changes in the Eastern Mediterranean freshwater
547 budget, using reconstructions of sea level and hydrography, *Proceedings Koninklijke Nederlandse*
548 *Akademie van Wetenschappen, Serie B*, 97, 201-217, 1994.
- 549 Rowan, J. S., Black, S., Macklin, M. G., Tabner, B. J., and Dore, J.: Quaternary environmental change
550 in Cyrenaica evidenced by U-Th, ESR and OSL of coastal alluvial fan sequences, *Libyan Studies*, 31,
551 5-16, 2000.



- 552 Schwarcz, H. P., Harmon, R. S., Thompson, P., and Ford, D. C.: Stable isotope studies of fluid
553 inclusions in speleothems and their paleoclimatic significance, *Geochimica et Cosmochimica Acta*,
554 40, 657-665, [http://dx.doi.org/10.1016/0016-7037\(76\)90111-3](http://dx.doi.org/10.1016/0016-7037(76)90111-3), 1976.
- 555 Smith, J. R., Giegengack, R., Schwarcz, H. P., McDonald, M. M. A., Kleindienst, M. R., Hawkins, A. L.,
556 and Churcher, C. S.: A reconstruction of quaternary pluvial environments and human occupations
557 using stratigraphy and geochronology of fossil-spring tufas, Kharga Oasis, Egypt, *Geoarchaeology-an*
558 *International Journal*, 19, 407-439, 2004.
- 559 Spötl, C.: Long-term performance of the Gasbench isotope ratio mass spectrometry system for the
560 stable isotope analysis of carbonate microsamples, *Rapid Communications in Mass Spectrometry*,
561 25, 1683-1685, [10.1002/rcm.5037](https://doi.org/10.1002/rcm.5037), 2011.
- 562 Swezey, C.: Eolian sediment responses to late Quaternary climate changes: temporal and spatial
563 patterns in the Sahara, *Palaeogeography, Palaeoclimatology, Palaeoecology*, 167, 119-155, 2001.
- 564 Toucanne, S., Angue Minto'o, C. M., Fontanier, C., Bassetti, M.-A., Jorry, S. J., and Jouet, G.: Tracking
565 rainfall in the northern Mediterranean borderlands during sapropel deposition, *Quaternary Science*
566 *Reviews*, 129, 178-195, <http://dx.doi.org/10.1016/j.quascirev.2015.10.016>, 2015.
- 567 Tuenter, E., Weber, S. L., Hilgen, F. J., and Lourens, L. J.: The response of the African summer
568 monsoon to remote and local forcing due to precession and obliquity, *Global and Planetary Change*,
569 36, 219-235, 2003.
- 570 Vaks, A., Woodhead, J., Bar-Matthews, M., Ayalon, A., Cliff, R., Zilberman, T., Matthews, A., and
571 Frumkin, A.: Pliocene–Pleistocene climate of the northern margin of Saharan–Arabian Desert
572 recorded in speleothems from the Negev Desert, Israel, *Earth and Planetary Science Letters*, 368, 88-
573 100, 2013.
- 574 Van Breukelen, M., Vonhof, H., Hellstrom, J., Wester, W., and Kroon, D.: Fossil dripwater in
575 stalagmites reveals Holocene temperature and rainfall variation in Amazonia, *Earth and Planetary*
576 *Science Letters*, 275, 54-60, 2008.
- 577 Wainer, K., Genty, D., Blamart, D., Daëron, M., Bar-Matthews, M., Vonhof, H., Dublyansky, Y., Pons-
578 Branchu, E., Thomas, L., van Calsteren, P., Quinif, Y., and Caillon, N.: Speleothem record of the last
579 180 ka in Villars cave (SW France): Investigation of a large $\delta^{18}O$ shift between MIS6 and MIS5,
580 *Quaternary Science Reviews*, 30, 130-146, <http://dx.doi.org/10.1016/j.quascirev.2010.07.004>, 2011.
- 581 Wassenburg, J. A., Immenhauser, A., Richter, D. K., Niedermayr, A., Riechelmann, S., Fietzke, J.,
582 Scholz, D., Jochum, K. P., Fohlmeister, J., Schröder-Ritzrau, A., Sabaoui, A., Riechelmann, D. F. C.,
583 Schneider, L., and Esper, J.: Moroccan speleothem and tree ring records suggest a variable positive
584 state of the North Atlantic Oscillation during the Medieval Warm Period, *Earth and Planetary Science*
585 *Letters*, 375, 291-302, <http://dx.doi.org/10.1016/j.epsl.2013.05.048>, 2013.
- 586 Wassenburg, J. A., Dietrich, S., Fietzke, J., Fohlmeister, J., Jochum, K. P., Scholz, D., Richter, D. K.,
587 Sabaoui, A., Spötl, C., Lohmann, G., Andreae, Meinrat O., and Immenhauser, A.: Reorganization of
588 the North Atlantic Oscillation during early Holocene deglaciation, *Nat. Geosci.*, 9, 602,
589 [10.1038/ngeo2767](https://doi.org/10.1038/ngeo2767)
- 590 <https://www.nature.com/articles/ngeo2767#supplementary-information>, 2016.

591

592 Figure Captions

593 Figure 1: Map showing the location of Susah Cave (filled circle) and GNIP sites used in the discussion
594 (open circles).

595 Figure 2) Macroscopic structure of SC-06-01 speleothem, showing alternation of transparent and
596 milky fabrics

597 Figure 3) Variability of water content (μL) per unit mass of speleothem (g) in SC-06-01 fluid inclusion
598 samples. Grey area shows working range of instrument.



599 Figure 4a) Fluid inclusion oxygen isotope values ($\delta^{18}\text{O}_{\text{fi}}$; blue crosses) compared to calcite oxygen
600 isotope values ($\delta^{18}\text{O}_{\text{cc}}$; black circles and line); 4b) Fluid inclusion hydrogen isotope values ($\delta^2\text{H}_{\text{fi}}$; blue
601 crosses) compared to $\delta^{18}\text{O}_{\text{cc}}$ (black circles and line). Growth Phases I, II and III are shown as grey
602 areas.

603 Figure 5a) Regional precipitation isotope data. Thick line represents Global Meteoric Water Line,
604 dashed thick line represents Mediterranean Meteoric Water Line and thin lines representing
605 expected range of deviation ($\pm 10\text{‰}$ $\delta^2\text{H}_{\text{ppt}}$) below GMWL and above MMWL. Bet Dagan, Tunis and
606 Sfax GNIP datasets (http://www-naweb.iaea.org/napc/ih/IHS_resources_gnip.html). Sfax Atlantic
607 and Mediterranean Rainfall are taken from Celle-Jeanton et al. (2003). 5b) Summarised precipitation
608 isotopes, and fluid inclusion measurements for SC-06-01.

609 Figure 6) Double-replicated fluid inclusion measurements from SC-06-01, and regional precipitation
610 isotope trends.

611 Figure 7) $^{87}\text{Sr}/^{86}\text{Sr}$ record for SC-06-01, compared to calcite $\delta^{18}\text{O}_{\text{cc}}$ record (light grey line). Error bars
612 are 2σ . Growth Phases I, II and III are shown as grey areas.

613 Figure 8) Carbon isotope ($\delta^{13}\text{C}_{\text{cc}}$) record for SC-06-01 compared to oxygen isotope record ($\delta^{18}\text{O}_{\text{cc}}$;
614 (Hoffmann et al., 2016)). Growth Phases I, II and III are shown as grey areas.

615 Figure 9) Fluid inclusion measurements relative to summarised precipitation data and the modern
616 precipitation end members used in the discussion. Solid lines are the Meteoric Water Lines as in Fig.
617 5a. Precipitation and fluid inclusion measurements are as shown in Figure 5b. “Mean Atlantic”, “Sfax
618 Mixed”, “Sfax Med” and “High Precip Atlantic” indicate the mean of measurements in Celle-Jeanton
619 et al (2003) originating from Atlantic moisture, mixed source, Mediterranean moisture and High
620 Precipitation measurements from an Atlantic moisture source (as described in Discussion)
621 respectively. “Mean Bet Dagan” is the mean of GNIP measurements from this location, and “High
622 Precip Bet Dagan” is the subset of high precipitation measurements as described in the Discussion.

623 Figure 10) Fluid inclusion deuterium excess ($\delta^2\text{H}_{\text{excess-Fi}}$) relative to calcite $\delta^{18}\text{O}_{\text{cc}}$. Note some fluid
624 inclusions (70 to 60 ka BP and 40 to 30 ka BP) show high $D_{\text{excess-Fi}}$ indicative of an Eastern
625 Mediterranean source. Growth Phases I, II and III are shown as grey areas.

626

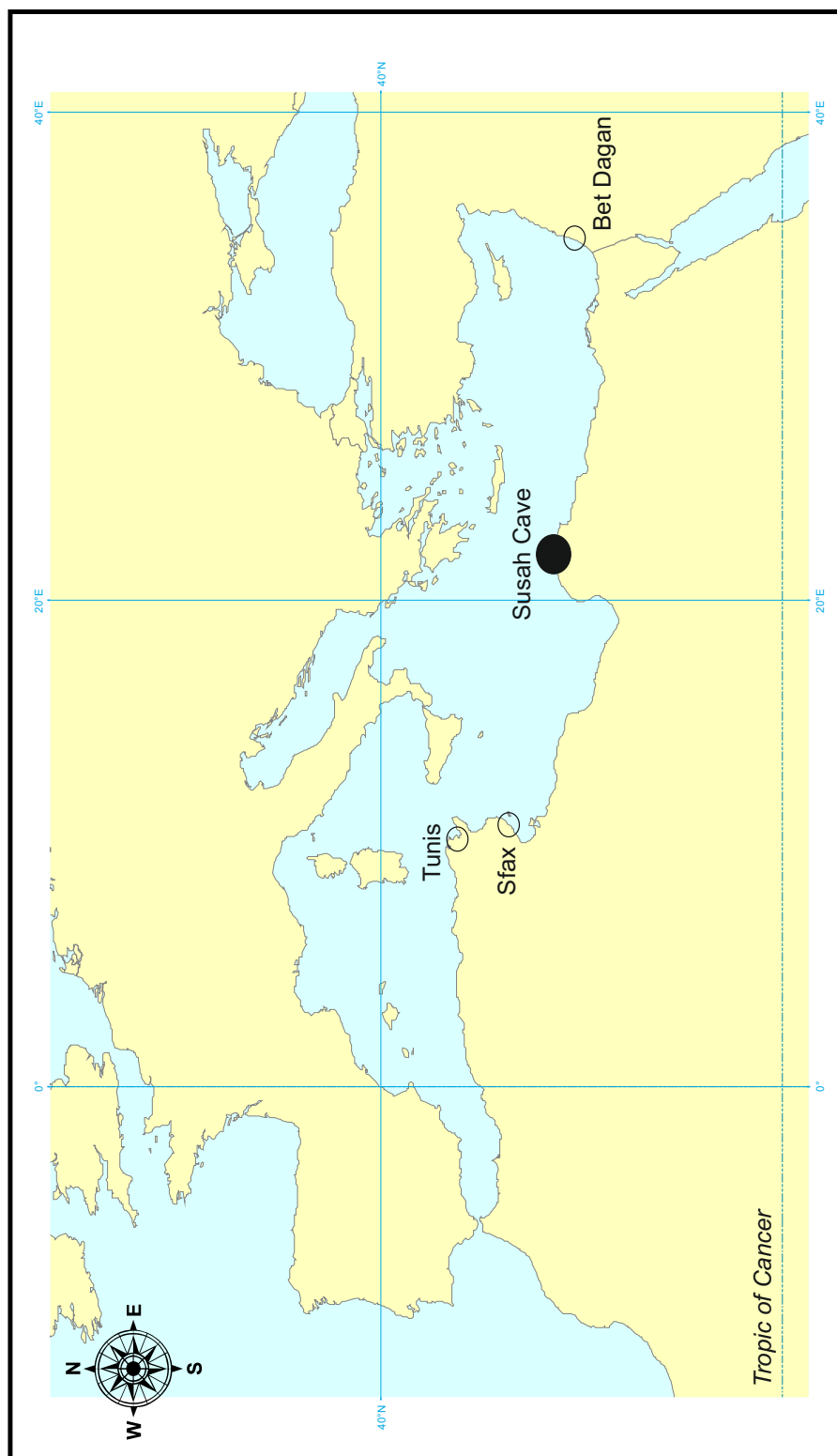




Figure 2

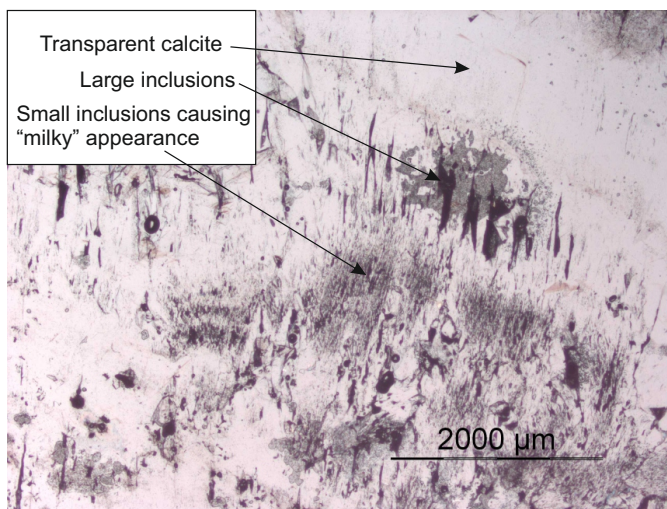




Figure 3

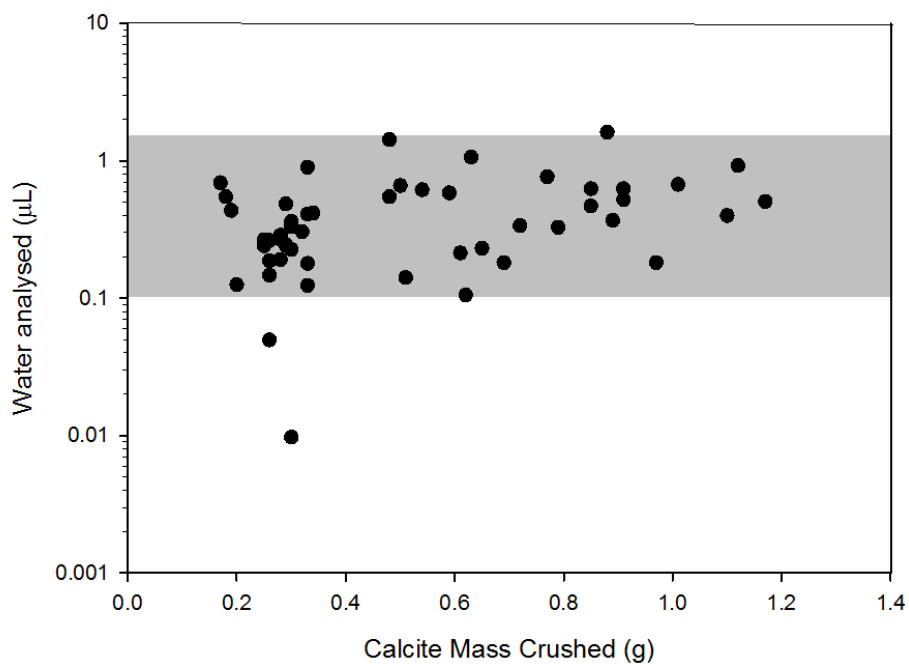




Figure 4a

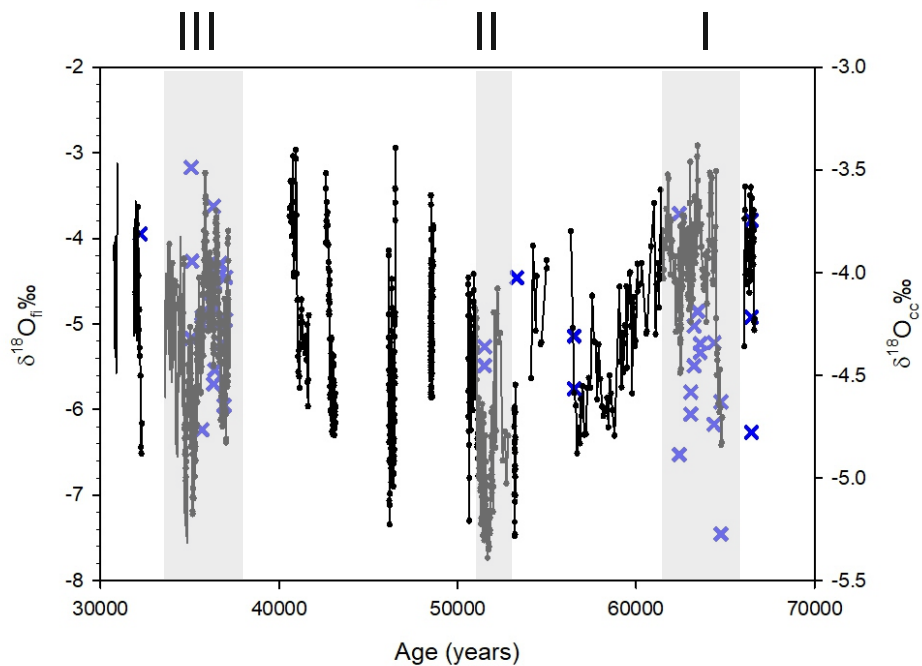


Figure 4b

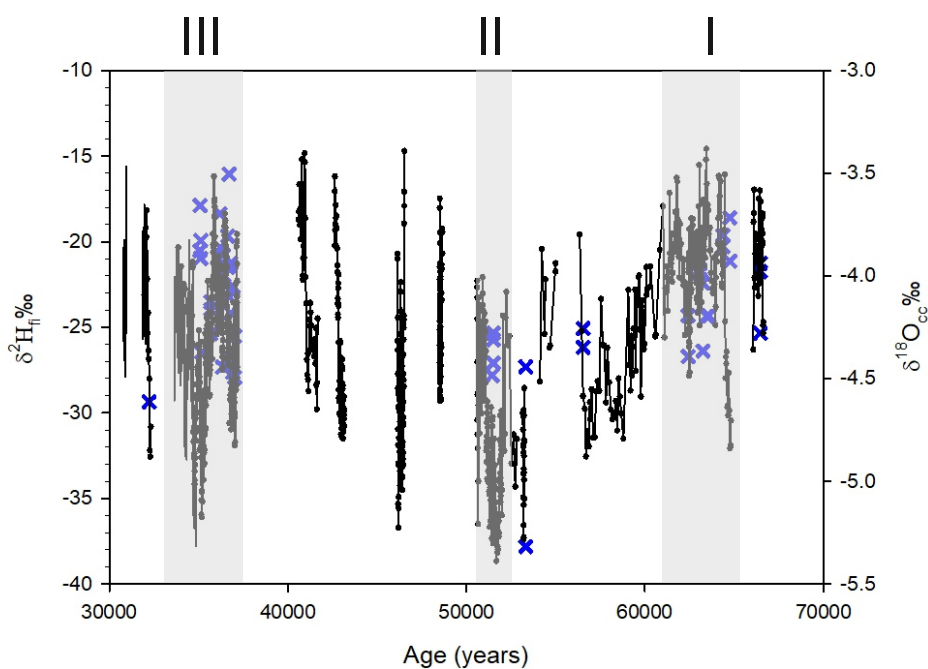




Figure 5a

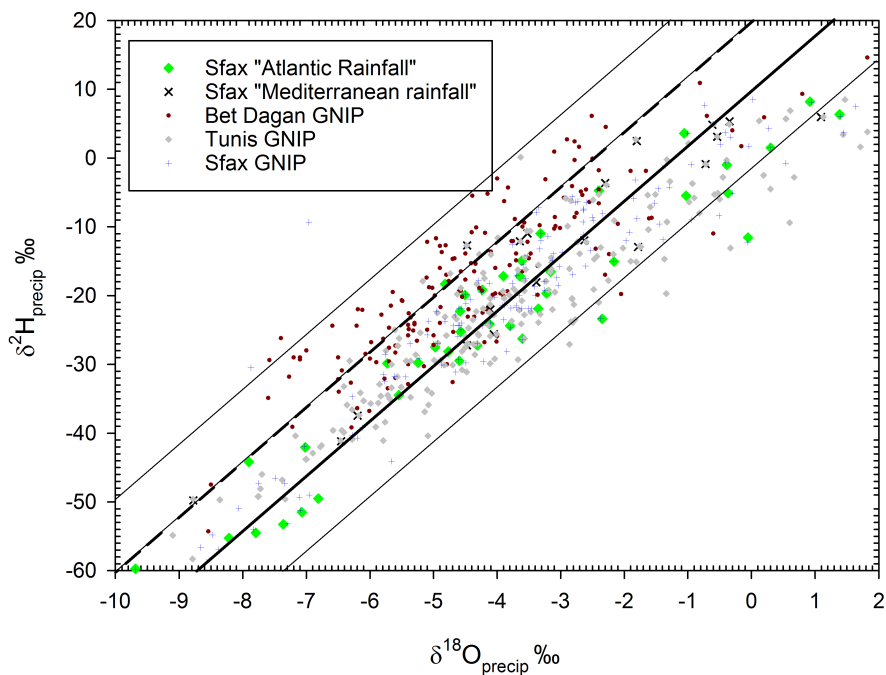


Figure 5b

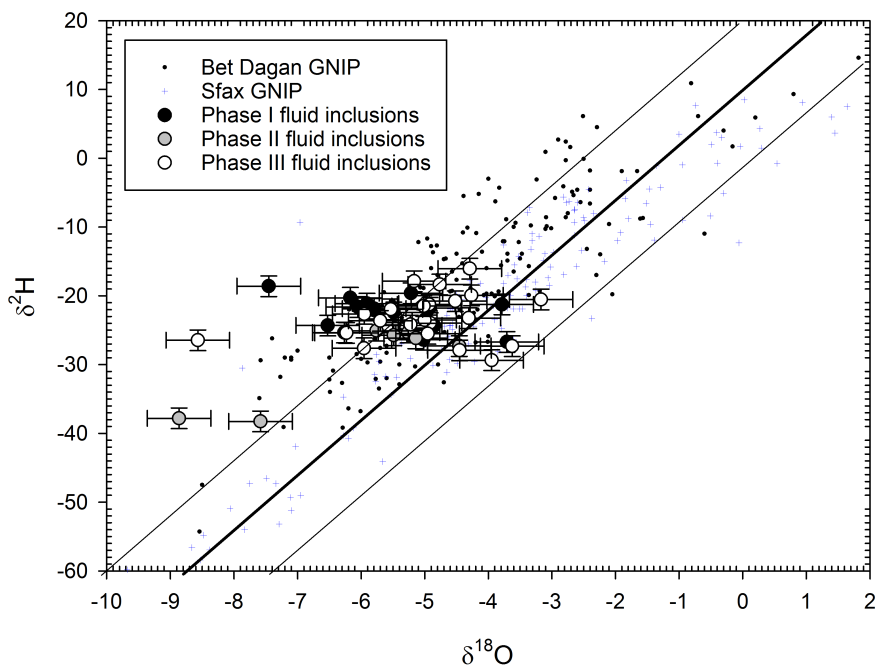
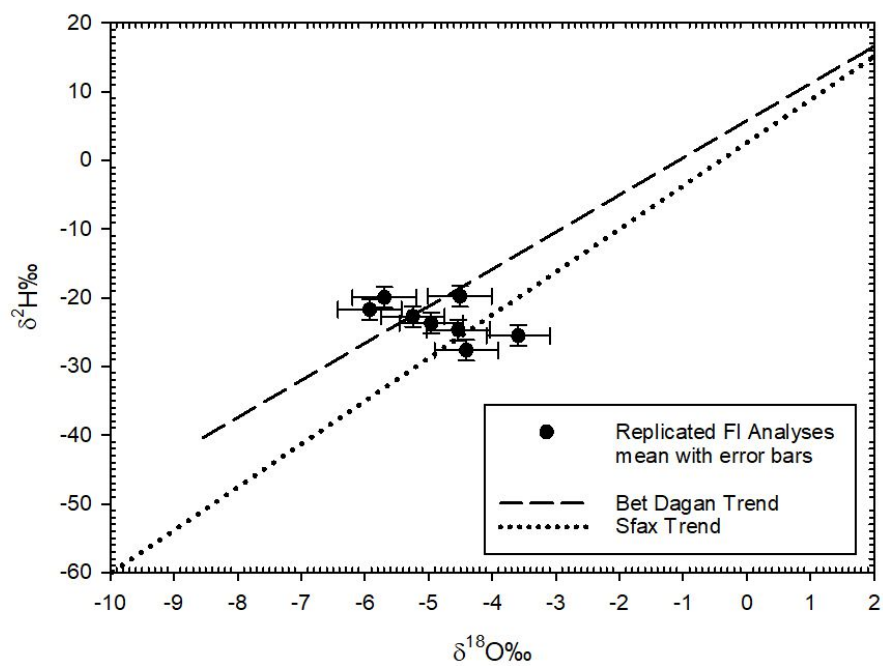
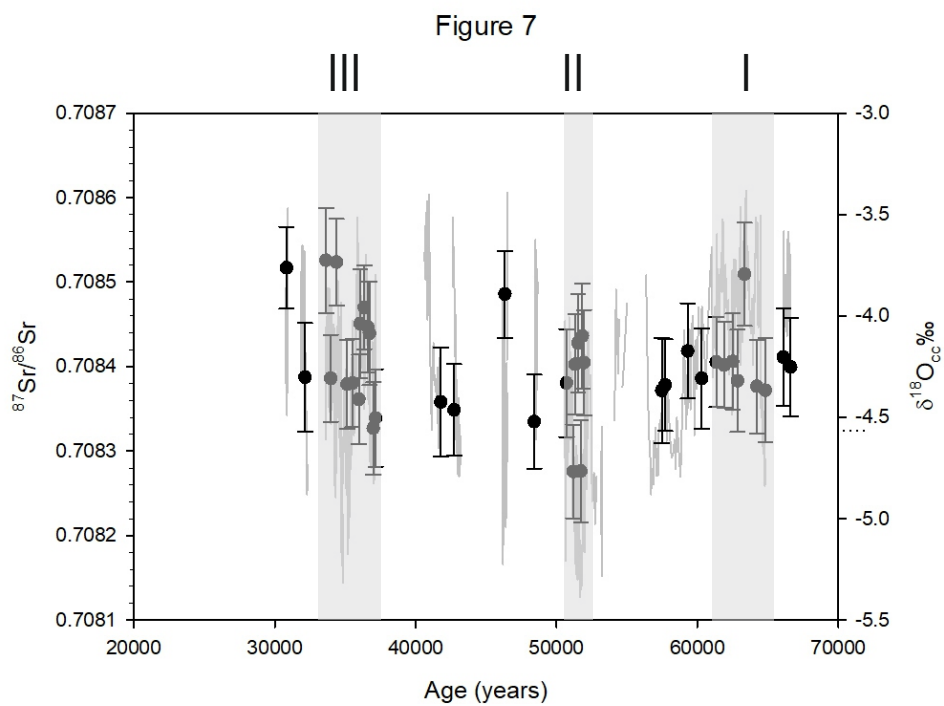




Figure 6





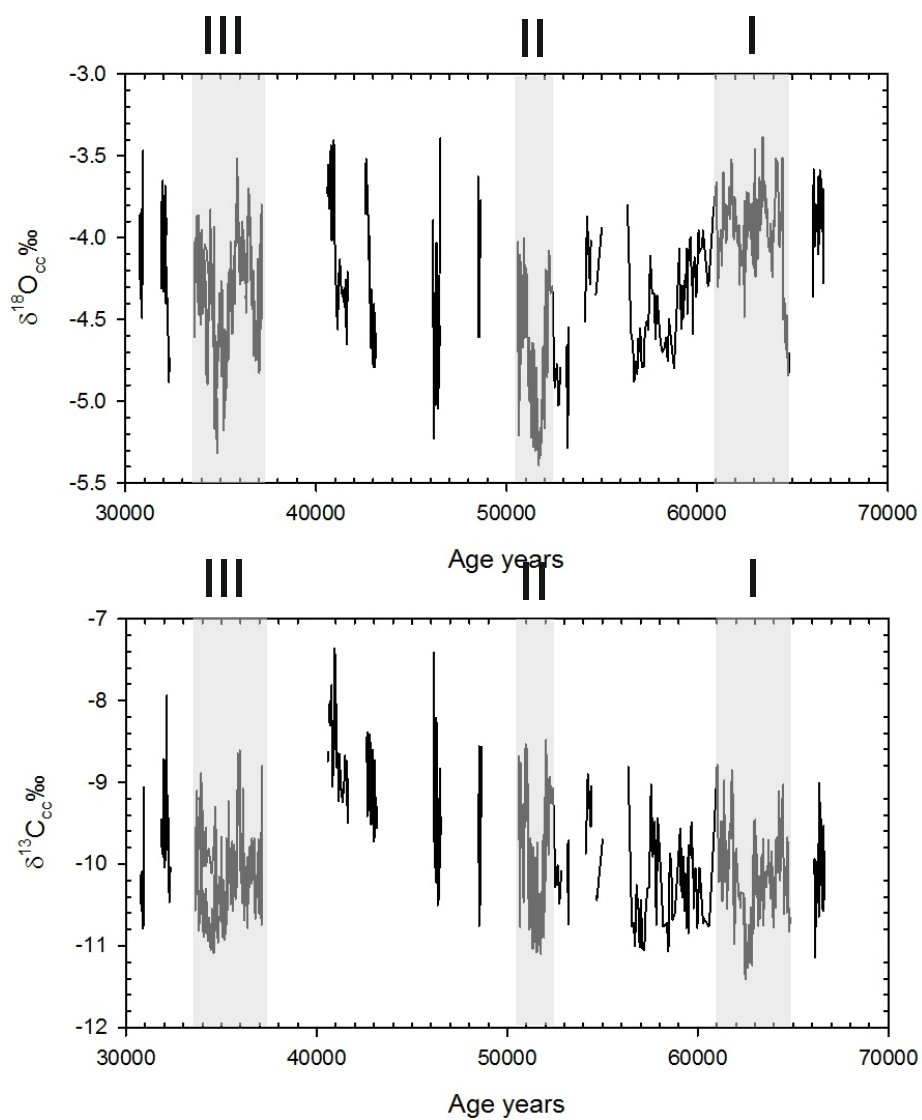




Figure 9

